Física Experimental I (FIS111)

Prof. Rodrigo B. Capaz

Instituto de Física

Universidade Federal do Rio de Janeiro

Informações Gerais

Webpage: http://www.if.ufrj.br/~msalves/fisexp1.html

Professor: Rodrigo Capaz (capaz@if.ufrj.br), Sala: A-432

Coordenador: Marcelo Alves (msalves@if.ufrj.br)

Monitoria: Horários a confirmar (ver webpage)

Texto: "Roteiros de Física Experimental I" (disponível na xerox do 3o. andar)

Regras do Curso

CRITÉRIO DE APROVAÇÃO E FREQUÊNCIA

✓ A avaliação dos alunos no curso de Física Experimental I é formada por duas notas parciais, N1 e N2.;
✓ cada nota parcial é formada pela média dos relatórios (20%) e prova individual (80%);
✓ a nota final é obtida pela média aritmética entre P1 e P2

$$NF = (N1 + N2)/2$$
$$NF \geq 5{,}0 \Rightarrow \text{APROVADO}$$
$$NF < 5{,}0 \Rightarrow \text{REPROVADO.}$$

- IMPORTANTE: NÃO HÁ PROVA FINAL OU QUALQUER OUTRA NOTA ALÉM DE P1 E P2;

FREQUÊNCIA

✓ A frequência nas aulas de Física Experimental é OBRIGATÓRIA.
✓ São permitidas 3 (três) faltas, acima disto o aluno está reprovado por frequência (RF).
- IMPORTANTE: a entrada do aluno na sala de aula só será permitida até 15 minutos após o horário de início.

Cronograma

Atenção: Este cronograma é diferente daquele utilizado para as demais turmas da disciplina

Módulo 1: A Descrição do Movimento

Módulo 2: As Leis do Movimento

Módulo 3: Trabalho e Energia

Módulo 4: Sistema de Partículas – Momento Linear

Módulo 5: Introdução à Estatística

Módulo 6: Rolamento e Corpos Rígidos

	SEGUNDA	QUARTA
OUTUBRO	15 Mod.1	17 Mod.1
	22 Mod.1/2	24 Mod.1/2
	29 Mod.2	31 Mod.2
NOVEMBRO	5 Mod.3	7 Mod.3
	12 Mod.3	14 Mod.3
	19 XXXXX	21 AVAL. 1
	26 AVAL.1	28 AVAL.1
DEZEMBRO	3 AVAL.1	5 Mod. 4
	10 Mod. 4	12 Mod. 4
	17 Mod. 4	19 XXXXX
FEVEREIRO	18 Mod. 5	20 Mod. 5
	25 Mod. 5/6	27 Mod. 5/6
MARÇO	4 Mod. 6	6 Mod. 6
	11 AVAL. 2	13 AVAL. 2

A natureza da Física

A Física é uma ciência experimental: A “resposta” da Natureza é o veredito supremo de uma teoria física.

Oposto ao idealismo de Hegel, que na sua dissertação de 1801, "As Órbitas dos Planetas", demonstrava que não podia existir mais do que sete planetas; e, se isso contrariasse os fatos, pior para os fatos...

A “arte” da Física está em:
1. O que e como perguntar à Natureza (experimento)?
2. Como interpretar suas respostas (teoria)?

O diálogo entre teoria e experimento é coordenado pelo MÉTODO CIENTÍFICO

O MÉTODO CIENTÍFICO

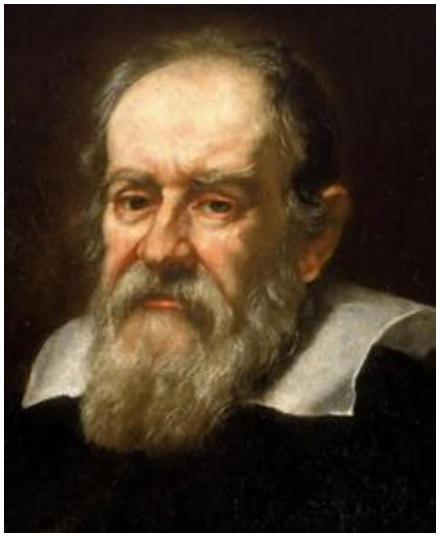

Galileu Galilei
(1564-1642)

OBSERVAÇÃO

↓

EXPERIMENTAÇÃO

↓

MODELAGEM

↓

PREVISÃO

Quando as previsões não são confirmadas pelas novas observações, a teoria está incorreta ou então as observações foram feitas fora de seu domínio de validade

Exemplo: Mecânica Clássica não é válida para objetos com velocidades próximas à da luz (Relatividade) ou na escala atômica (Mecânica Quântica)

Módulo 1 – A Descrição do Movimento

Objetivo: Determinar a velocidade de um carrinho que se desloca sobre um trilho de ar

O trilho de ar:

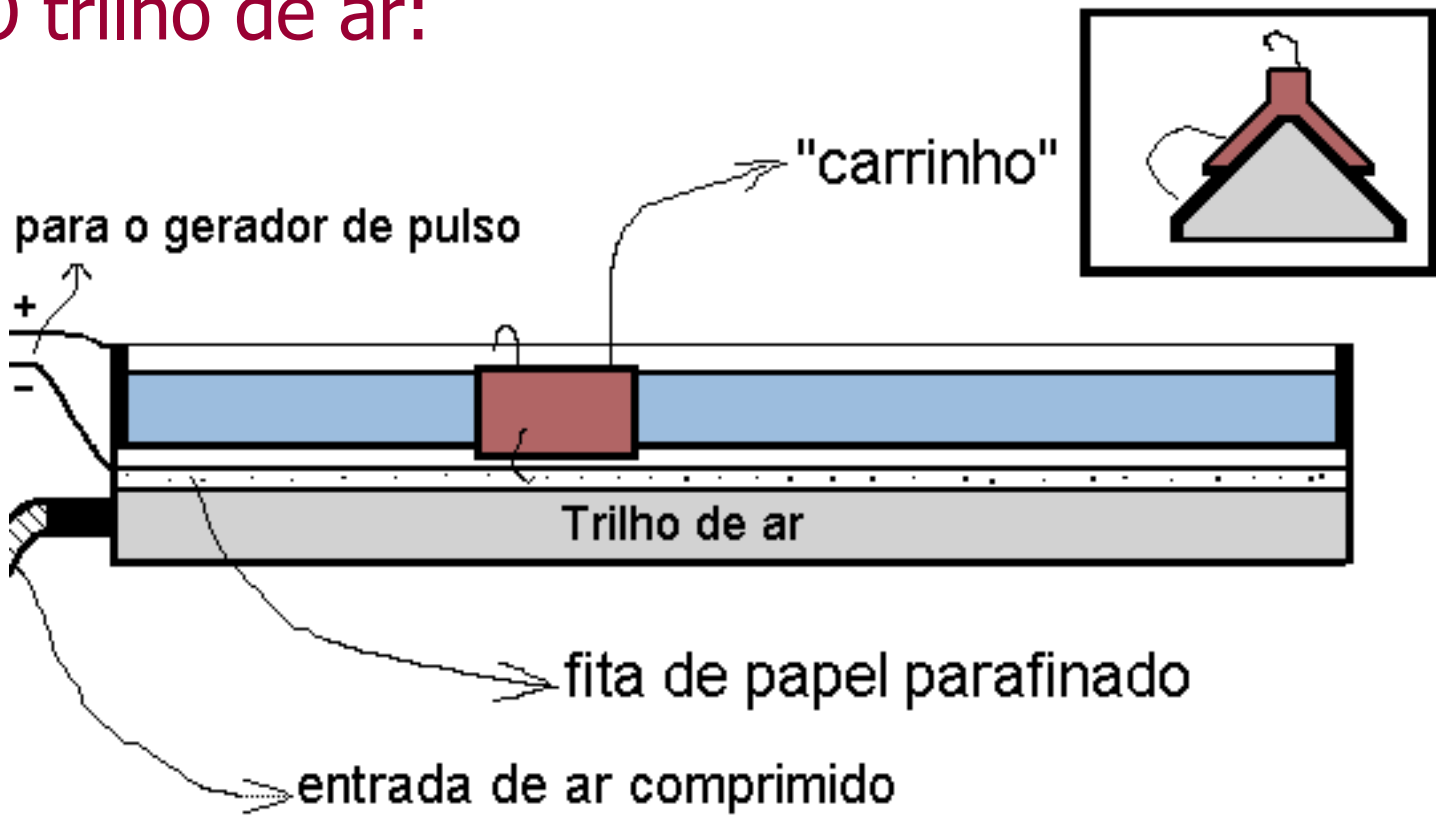

Procedimento experimental:

1. Nivelar o trilho de ar
2. Verificar a instalação elétrica do centelhador
3. Simular a obtenção dos dados
4. **Tomada de dados!**

Construir uma tabela de medidas de posição como função do tempo:

t (s)	x (cm)	δx (cm)
0,0	...	...
0,1	...	...
0,2	...	...

Incerteza na medida da posição.

O que é? Como determinar?

Padrões e unidades

Grandeza Física: "Propriedade de um fenômeno, corpo ou substância que pode ser expressa sob a forma de um número e uma referência (padrão)". *(VIM – Vocabulário Internacional de Termos Gerais e Fundamentais de Metrologia)*

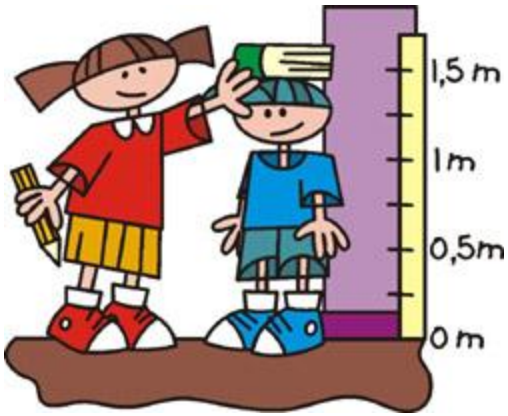

Exemplo: altura = 1,73 m

Valor

Unidade (definida através de um padrão)

Sistema de unidades: "Sistema Internacional (SI)"

Grandezas e Unidades Fundamentais do S.I.

Nome de grandeza	Símbolo de grandeza	Nome da unidade	Símbolo da unidade
Comprimento	l	metro	m
Massa	m	quilograma	kg
Tempo	t	segundo	s
Intensidade de corrente eléctrica	I	ampere	A
Temperatura	T	kelvin	K
Quantidade de matéria	n	mole	mol
Intensidade luminosa	I_v	candela	cd

Demais unidades podem ser obtidas a partir das unidades fundamentais

Exemplo: newton: $N = kg.m/s^2$

Incerteza e algarismos significativos

Toda medida física tem uma incerteza associada e o resultado só pode ser expresso até o último algarismo significativo.

Estação de trem de Rio Grande da Serra (SP): Altitude com precisão de milímetros!

Maneiras distintas de expressar a incerteza:

a. 56,47 ± 0,02 : valor real entre 56,45 e 56,49

b. 1,6454(21) = 1,6454 ± 0,0021

c. Fracionária ou percentual: 47 ± 10% = 47 ± 5

d. Implícita: 2,91 = 2,91 ± 0,01 (incerteza no último significativo)

Noção intuitiva de incerteza: "*Se repetir a medida novamente, tenho grande confiança de que o resultado encontrado estará dentro da faixa de incerteza*"

Exemplo: 56,47 ± 0,02 : grande confiança de que o valor medido novamente estará entre 56,45 e 56,49

Futuramente, veremos no curso que "grande confiança" tem um significado estatístico bem preciso...

Vamos explorar esse conceito através da medida do período de um pêndulo (cada aluno mede o período com um cronômetro e o professor coleta e analisa os resultados)

Agora estamos prontos para estimar a incerteza na medida da posição. Um valor razoável é $\delta x = 0{,}1$ cm

Modelo Teórico

Não há força resultante sobre o carrinho: aceleração nula

Movimento Retilíneo Uniforme: velocidade constante

$$v_x = v_{0x} = \text{constante}$$

$$x(t) = x_0 + v_{0x}t$$

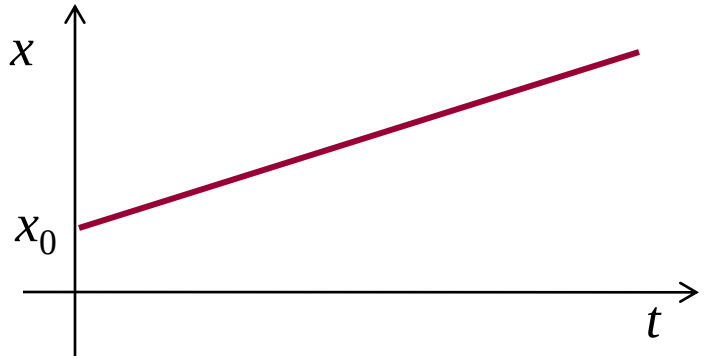

Vamos fazer o gráfico de x vs. t para comparar com o modelo teórico

Como fazer um gráfico?

PRL **109,** 155305 (2012) PHYSICAL REVIEW LETTERS week ending 12 OCTOBER 2012

Roton-Phonon Interactions in Superfluid ^{4}He

B. Fåk,[1] T. Keller,[2,3] M. E. Zhitomirsky,[1] and A. L. Chernyshev[4]

- Grandezas físicas e suas unidades identificadas nos eixos coordenados
- Valores marcados nos eixos em intervalos iguais
- Incertezas dos pontos experimentais identificadas com barras de erro
- O gráfico deve ocupar o maior espaço possível na folha de papel milimetrado

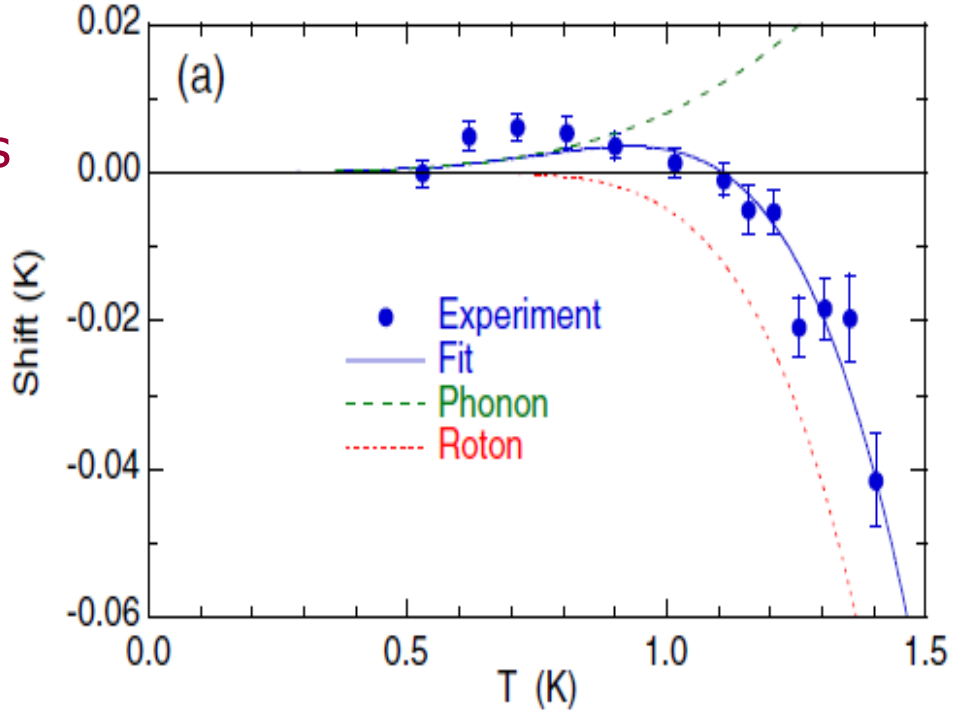

- Ao fazer um ajuste visual por uma curva ou reta, não privilegie nenhum dos pontos experimentais em detrimento dos demais. Encontre uma curva que passe próximo a todos ou à maioria dos pontos

(os alunos fazem o gráfico: fim da primeira aula)

Obtendo a velocidade do carrinho

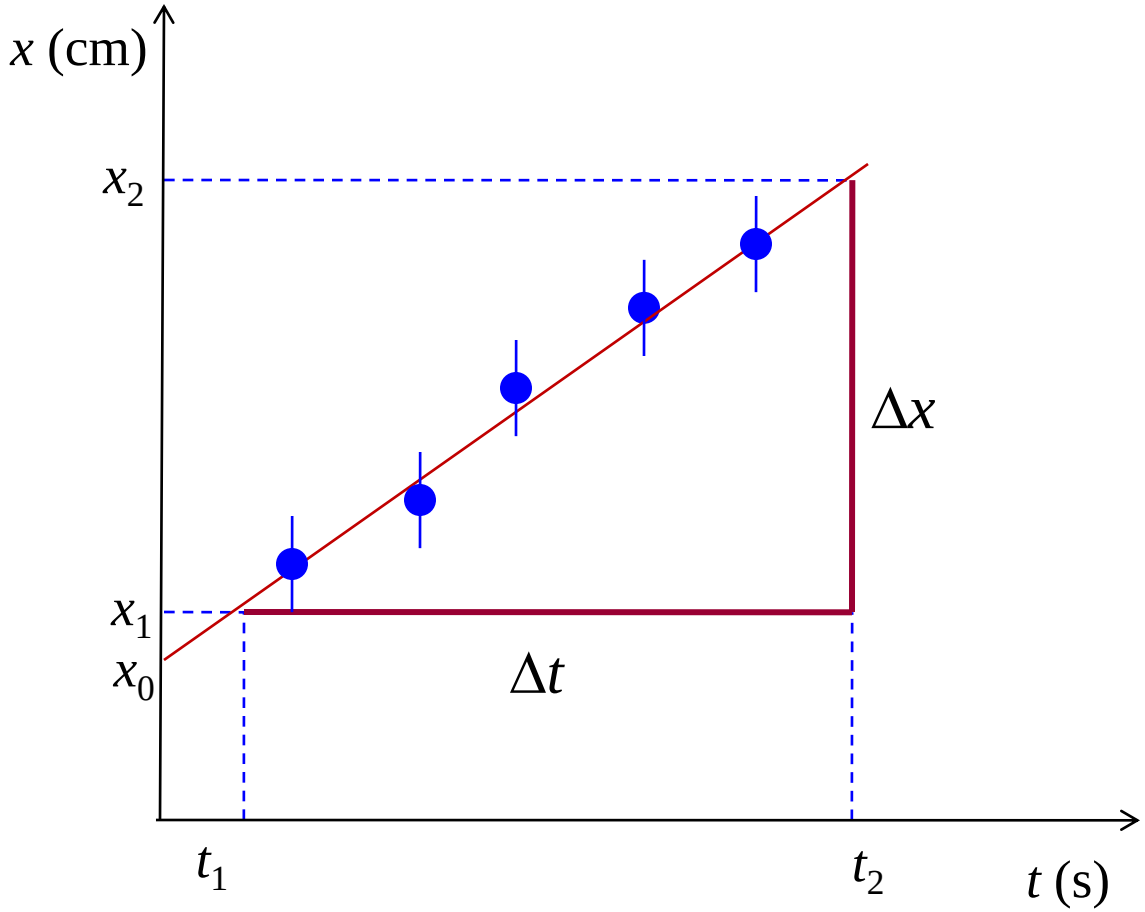

$$v_x = \frac{\Delta x}{\Delta t}$$

(velocidade instantânea é igual à velocidade média neste caso)

Como escrever um relatório?

O relatório é dividido em partes, não muito diferente de um artigo científico

Título da experiência

Autor

Introdução: objetivo da experiência

Procedimento experimental

PHYSICAL REVIEW B 86, 155202 (2012)

Origin of the significantly enhanced optical transitions in layered boron nitride

Bing Huang,[1] X. K. Cao,[2] H. X. Jiang,[2] J. Y. Lin,[2] and Su-Huai Wei[1]

[1]National Renewable Energy Laboratory, 1617 Cole Boulevard, Golden, Colorado 80401, USA

[2]Department of Electrical and Computer Engineering, Texas Tech University, Lubbock, Texas 79409, USA

(Received 24 February 2012; revised manuscript received 24 April 2012; published 1 October 2012)

It is normally expected that an excellent optical material should have $p \rightarrow s$-like transitions at the absorption edge. This is because the strength of $p \rightarrow s$-like transitions usually is much stronger than those of $p \rightarrow p$ transitions, especially in those ionic semiconductors where the electronic states are more localized and behave as atomic characters. Here, we demonstrate an exception that the luminescence intensity of hexagonal boron nitride (h-BN) could be at least two orders of magnitude greater than that of AlN, despite the dominated atomic $p \rightarrow p$ transitions at the absorption edge of h-BN. Using group theory analysis and first-principles calculations, we show that the strong optical transitions in h-BN originate from the unusually strong $p \rightarrow p$-like transitions and its "two-dimensional" nature. As learned from h-BN, we demonstrate that one can dramatically increase the absorption or luminescence intensity at the fundamental absorption edge of an optical material by confining its thickness into a few layers, which is much more effective than the commonly used superlattice technology.

DOI: 10.1103/PhysRevB.86.155202 PACS number(s): 78.66.−w, 71.15.Mb, 71.20.Nr, 78.20.−e

I. INTRODUCTION

The optical absorption coefficient $\alpha(\omega)$ and photoluminescent intensity $I(\omega)$ are mostly determined by the quantum transition rate $W_{i\rightarrow f}$ given by Fermi's golden rule $W_{i\rightarrow f} \propto |M|^2 g(\hbar\omega)$, where $|M|^2 = |\langle f|\vec{\varepsilon}\cdot\vec{p}|i\rangle|^2$ is the dipole matrix element square between states i and f, and $g(\hbar\omega)$ is the joint density of states[1,2] with $\hbar\omega = E_f - E_i$ where E_f and E_i are the energy of states f and i. In the textbook description, one learns that, in a spherically symmetric atom, an allowed optical electric-dipole transition requires that the orbital angular momentum l of the initial and final states differ by ± 1, i.e., atomic $p \rightarrow p$ transition is forbidden, but the $p \rightarrow s$ transition is expected to have large magnitude. When atoms form a crystal, due to reduced symmetry, even though this kind of $p \rightarrow p$ transition may not be completely forbidden, it is normally expected that the crystal inherits the atomic features: thus the strengths of $p \rightarrow p$-like transitions should be much weaker than those of $p \rightarrow s$ transitions, especially in those ionic semiconductors where the electronic states are more localized and behave as atomic characters. Until now, the preferred optical materials have been mostly those semiconductors with $p \rightarrow s$ transitions at the absorption edges. For example, group-III nitrides AlN, GaN, InN, and their alloys are widely used in solid-state lighting for ultraviolet (UV) and visible lights.[3]

AlN and its related materials play a dominant role in deep-UV applications due to their suitable band gaps and strong optical transition rates at the absorption edge.[3] Layered hexagonal BN (h-BN), although it has a band gap close to that of AlN, was initially not considered a good optical material because, as in most layered ionic semiconductors, its conduction and valence band edges both have atomic p_z characters. Therefore, it is quite unexpected that experimentally it has been shown that h-BN can exhibit high light-emitting intensity for deep-UV lasing and LED applications.[4] To develop future optical materials, it will be quite important to understand the fundamental origin of why h-BN could be a good emitter and what are the advantages of layered h-BN compared to other conventional high-efficiency optical materials such as AlN.

By employing experimental measurements and first-principles calculations, we demonstrate that atomic-like $p \rightarrow p$ transitions are not only allowed in h-BN due to reduced symmetry, but can also have very large transition rates due to the small B-N bond length, and thus large overlap between B and N p orbitals. The unusual $p \rightarrow p$ transitions combined with the large joint density of states of electron-hole pairs resulting from the "two-dimensional" nature of h-BN lead to a high absorption or luminescence intensity at the fundamental absorption edge, which is at least two orders of magnitude greater than that of AlN. As learned from h-BN, we demonstrate that the absorption or luminescence intensity at the fundamental absorption edge of an optical material can be largely enhanced by confining its thickness into a few layers.

II. EXPERIMENTAL AND COMPUTATIONAL METHODS

AlN epilayers are grown at 1200 °C using hydrogen as a carrier gas with a growth rate of about 1 μm/h. Epitaxial layers of h-BN are produced usin'g triethylboron (TEB) and ammonia (NH_3) as B and N sources, respectively. A thin BN buffer layer is deposited at 650 °C prior to the growth of the epilayer. h-BN epilayers are grown at 1300 °C using hydrogen as a carrier gas with a growth rate of 0.5 μm/hr. X-ray diffraction (XRD) measurements reveal that AlN and h-BN samples employed in this work have a full width at half maximum (FWHM) of ~400 arc sec for a (002) rocking curve. Photoluminescence (PL) signals are collected in two different configurations of the polarization of emitted light, e.g., the electrical field of the PL emission is directed either parallel ($\vec{\varepsilon}\|\vec{c}$) or perpendicular ($\vec{\varepsilon}\perp\vec{c}$) to the c axis. The PL spectra of h-BN and AlN are measured with identical conditions with two samples sitting side by side vertically, and PL data are collected for each by moving the samples through the use of a vertical translational stage. A frequency-quadrupled Ti-sapphire laser with a repetition rate of 76 MHz and 100 fs pulse width operating at 197 nm is focused onto the sample surface through a microscope objective. The collected PL signal is then dispersed by a 1.3 m monochromator and detected by a micro-channel-plate photomultiplier tube.

Modelo Teórico

Resultados: Tabelas e gráficos

All the density-functional-theory (DFT) calculations are performed by using the VASP code.[5] Projector augmented wave (PAW) potentials are used to describe the interaction of core and valence electrons, and a generalized gradient approximation (GGA) with the PBE functional is selected in our calculations. It is well known that GGA type calculations usually underestimate the band gaps of semiconductors, and hybrid functional calculations could give improved results for both conventional semiconductors, thus we adopt a hybrid functional[6] to calculate the electronic structures. A 20 Å vacuum region is included when we calculate the nanostructures. The pseudo-H method[7] is used to passivate the surfaces of BN quantum dot (QD), AlN thin film, and GaN thin film. Enough k-point sampling is used for the Brillouin-zone integration. The energy cutoff is set to 500 eV and structural optimization is carried out on all systems until the residual forces converge to 0.01 eV/Å. The detailed methods of optical calculations are described in Ref. 8. The symmetry related calculations and analysis are done in QUANTUM ESPRESSO code.[9] Moreover, the GW correction and Bethe-Salpeter equation calculations are carried out in YAMBO project code.[10] For the calculations performed with the YAMBO code, the ground-state Kohn-Sham wave functions and eigenvalues are obtained using a local-density approximation (LDA) exchange-correlation functional with Troullier-Martins norm-conserving pseudopotentials, as implemented in QUANTUM ESPRESSO code. A kinetic energy cutoff of 100 Ry is used for the wave function. These calculations are carried out to obtain an input compatible with the YAMBO code.

III. RESULTS AND DISCUSSION

Epitaxial AlN and h-BN with thicknesses of ~1.0 μm are synthesized by metal-organic chemical-vapor deposition on (0001) sapphire substrates. The PL spectra of h-BN and AlN are measured with identical conditions with two samples sitting side by side vertically, and PL data are collected for each by moving the samples through the use of a vertical translational stage. As shown in Fig. 1, the PL measurements show that the peak intensity of h-BN along $\vec{e}\perp\vec{c}$ is about twice as large as $\vec{e}\parallel\vec{c}$. In contrast to h-BN, the emission along $\vec{e}\perp\vec{c}$ in AlN is almost forbidden (a very small angle in collection configuration makes the recorded $I_{\rm emi}$ of AlN nonzero along $\vec{e}\perp\vec{c}$). Surprisingly, we find that the emission from h-BN is at least 400 times greater (peak intensity) than that of AlN from the allowed transitions. This is unusual because the strength of the $p \rightarrow s$ transition at the AlN absorption edge is expected to be much stronger than that of the atomic-like $p \rightarrow p$ transition in h-BN. Therefore, an interesting question is why strong optical transition rates can exist in h-BN.

In order to investigate the strong optical transitions in h-BN, we have studied the possibility and strengths of $p \rightarrow p$ transitions in BN structures. BN is known to have three different crystal structures: cubic zinc-blende BN (c-BN), hexagonal wurzite BN (w-BN), and h-BN.[11] We first examine the probability of $p \rightarrow p$ transitions in these BN structures by using the general group theory analysis, and then we calculate the size of $|M|^2$ for the $p \rightarrow p$ transitions. In the following, we will focus on the electron-dipole transitions at the Γ point where the symmetry is the same as that of the crystal.

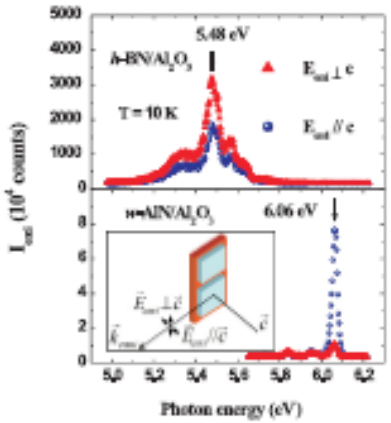

FIG. 1. (Color online) The PL emission spectra of h-BN and w-AlN epilayers grown on sapphire substrate by metal-organic chemical-vapor deposition, which is collected in the configuration of the electrical field of emission perpendicular ($\vec{E}\perp\vec{c}$) and parallel ($\vec{E}\parallel\vec{c}$) to the c axis, respectively, controlled through the use of a polarizer in front of the monochromator.

In a zinc-blende crystal (T_d symmetry), $\vec{P}$ belongs to a Γ_{15}[12,13] irreducible representation and the matrix element is isotropic. Our calculations show that for sp semiconductors the representations of the four valence bands are Γ_1 and Γ_{15}, with Γ_{15} as the valence-band maximum. The wave functions generated from the operation of $\vec{P}$ on Γ_{15} states can be reduced to a direct sum of irreducible representations, i.e., $\vec{P}|\Gamma_{15}\rangle = \Gamma_1 \oplus \Gamma_{12} \oplus \Gamma_{15} \oplus \Gamma_{25}$. In terms of the matrix-element theory, this indicates that dipole transitions from a Γ_{15} valence band are only allowed to conduction bands with Γ_1, Γ_{12}, Γ_{15}, or Γ_{25} symmetries (Table I). Thus, like the $p \rightarrow s$ ($\Gamma_{15} \rightarrow \Gamma_1$) transition, the $p \rightarrow p$ ($\Gamma_{15} \rightarrow \Gamma_{15}$) transition is also allowed. Our calculations show that, surprisingly, the strength of the $p \rightarrow p$ ($|\langle\Gamma_{15}|\vec{e}\cdot\vec{P}|\Gamma_{15}\rangle|^2 = 1.13$) transition is comparable to that of the $p \rightarrow s$ ($|\langle\Gamma_1|\vec{e}\cdot\vec{P}|\Gamma_{15}\rangle|^2 = 1.24$)

TABLE I. Symmetry analysis of the representations of the momentum operator, the top of the valence band wave functions, and the direct product $\vec{P}|v\rangle$ at the Γ point, which determines the conduction band states that can have allowed dipole transition for T_d, C_{6v}, and D_{6h} symmetries.

Symmetry	$\vec{P}$	$\|v\rangle$	$\vec{P}\|v\rangle$
T_d	Γ_{15}	Γ_{15}	$\Gamma_1 \oplus \Gamma_{12} \oplus \Gamma_{15} \oplus \Gamma_{25}$
C_{6v}	Γ_6 ($\vec{e}\perp\vec{c}$)	Γ_6	$\Gamma_1 \oplus \Gamma_2 \oplus \Gamma_5$
	Γ_1 ($\vec{e}\parallel\vec{c}$)	Γ_6	Γ_6
	Γ_6 ($\vec{e}\perp\vec{c}$)	Γ_1	Γ_6
	Γ_1 ($\vec{e}\parallel\vec{c}$)	Γ_1	Γ_1
D_{6h}	Γ_6^- ($\vec{e}\perp\vec{c}$)	Γ_6^-	$\Gamma_1^+ \oplus \Gamma_2^+ \oplus \Gamma_5^+$
	Γ_2^- ($\vec{e}\parallel\vec{c}$)	Γ_6^-	Γ_6^+
	Γ_6^- ($\vec{e}\perp\vec{c}$)	Γ_2^-	Γ_6^+
	Γ_2^- ($\vec{e}\parallel\vec{c}$)	Γ_2^-	Γ_1^+

Conclusões: os resultados da experiência confirmam a previsão teórica? Caso contrário, porque não?

"quantum" optical properties can be achieved. For example, from the Bohr effective mass model we can roughly estimate that the critical quantum thicknesses for AlN and GaN are around 1.8 and 3.1 nm, respectively. The calculated ε_2 of a 4-layer (~1 nm) GaN and AlN thin slabs are shown in Figs. 4(a) and 4(b). Obviously, a large enhanced absorption intensity can be realized in the GaN and AlN thin slabs. When the thickness of the thin slab is increased, the quantum size effect becomes weaker and the absorption or luminescence intensity at the absorption edge is decreased and close to that of bulk. For example, a 10-layer GaN thin slab with a thickness of ~3.5 nm exhibits an absorption spectrum similar to that of bulk GaN. More interestingly, our calculations indicate that the widely used superlattice structures (such as 20-layer-AlN/4-layer-GaN/20-layer-AlN)[3] cannot achieve a large improvement in the absorption intensity of GaN compared to the thin slab we proposed, as shown in Fig. 4(a), mainly because the electron potential barrier induced by the AlN layers (~2 eV) is not high enough to realize a "real" 2D effect. Our understandings can also explain well the recent experimental observations that significant enhancements of absorption or luminescence intensity can be achieved in CdX (X = Se, S, or Te) thin films only when their thicknesses are limited to a few layers.[24]

IV. CONCLUSION

In conclusion, by combining first-principles calculations and experiments, we have addressed the question why h-BN could be a brighter emitter than AlN. The understanding of the unusual property in h-BN also suggests that the absorption or luminescence intensity at the fundamental absorption edge of an optical material can be greatly enhanced by confining its thickness into a few layers, which is more effective than the commonly used superlattice technology.

ACKNOWLEDGMENTS

This work was supported by the US Department of Energy under Contract No. DE-AC36-08GO28308 to NREL and under Contract No. FG02-09ER46552 to TTU. H.X.J. and J.Y.L. would like to acknowledge the support of Whitacre endowed chair positions through the AIT foundation. We would also like to acknowledge assistance from Qiang Xu of NREL and J. Li and S. Majety from TTU.

[1] M. L. Cohen and J. R. Chelikowsky, *Electronic Structure and Optical Properties of Semiconductors* (Springer-Verlag, Berlin, 1988).

[2] P. Y. Yu and M. Cardona, *Fundamentals of Semiconductors: Physics and Materials Properties* (Springer-Verlag, Berlin, 2001).

[3] *Handbook of Luminescent Semiconductor Materials*, edited by L. Bergman and J. L. McHale (Taylor Francis Group, Boca Raton, FL, 2011).

[4] K. Watanabe, T. Taniguchi, and H. Kanda, Nat. Mater. **3**, 404 (2004); Y. Kubota, K. Watanabe, O. Tsuda, and T. Taniguchi, Science **317**, 932 (2007); K. Watanabe, T. Taniguchi, and H. Kanda, Nat. Photon. **3**, 591 (2009); R. Dahal, J. Li, S. Majety, B. N. Pantha, X. K. Cao, J. Y. Lin, and H. X. Jiang, Appl. Phys. Lett. **98**, 211110 (2011).

[5] G. Kresse and J. FurthmAuller, Comput. Mater. Sci. **6**, 15 (1996).

[6] J. Heyd, G. E. Scuseria, and M. Ernzerhof, J. Chem. Phys. **118**, 8207 (2003).

[7] B. Huang, Q. Xu, and S.-H. Wei, Phys. Rev. B **84**, 155406 (2011).

[8] M. Gajdos, K. Hummer, G. Kresse, J. Furthmuller, and F. Bechstedt, Phys. Rev. B **73**, 045112 (2006).

[9] P. Giannozzi *et al.*, J. Phys.: Condens. Matter **21**, 395502 (2009).

[10] A. Marini, C. Hogan, M. Gruning, and D. Varsano, Comput. Phys. Commun. **180**, 1392 (2009).

[11] *Properties of Group III Nitrides*, edited by J. H. Edgar (INSPEC, London, 1994).

[12] The irreducible representations are labeled according to the notations of G. F. Koster, J. O. Dimmock, R. G. Wheeler, and H. Statz, *Properties of the Thirty-two Point Groups* (MIT Press, Cambridge, MA, 1963).

[13] R. H. Parmenter, Phys. Rev. **100**, 573 (1955).

[14] G. D. Chen, M. Smith, J. Y. Lin, H. X. Jiang, S.-H. Wei, M. A. Khan, and C. J. Sun, Appl. Phys. Lett. **68**, 2784 (1996).

[15] J. Li, K. B. Nam, M. L. Nakarmi, J. Y. Lin, H. X. Jiang, P. Carrier, and S.-H. Wei, Appl. Phys. Lett. **83**, 5163 (2003).

[16] The spin-orbital coupling can mix Γ_6 and Γ_1 states. For simplicity of symmetry analysis, we assume here the spin-orbital splitting is much smaller than the crystal field splitting, which is true for AlN and BN.

[17] H. W. Streitwolf, Phys. Status Solidi **33**, 225 (1969).

[18] R. L. Benbow, Phys. Rev. B **22**, 3775 (1980).

[19] Y.-N. Xu and W. Y. Ching, Phys. Rev. B **44**, 7787 (1991); N. E. Christensen and I. Gorczyca, *ibid.* **50**, 4397 (1994); X. Blase, A. Rubio, S. G. Louie, and M. L. Cohen, *ibid.* **51**, 6868 (1995).

[20] *Synthesis and Properties of Boron Nitride*, edited by J. J. Pouch and S. A. Alterovitz (Trans Tech, Switzerland, 1990).

[21] L. Song, L. Ci, H. Lu, P. B. Sorokin, C. Jin, J. Ni, A. G. Kvashnin, D. G. Kvashnin, J. Lou, B. I. Yakobson, and P. M. Ajayan, Nano Lett. **10**, 3209 (2010); Y. M. Shi, C. Hamsen, X. T. Jia, K. K. Kim, A. Reina, M. Hofmann, A. L. Hsu, K. Zhang, H. N. Li, Z. Y. Juang, M. S. Dresselhaus, L. J. Li, and J. Kong, *ibid.* **10**, 3209 (2010); K. K. Kim, A. Hsu, X. Jia, S. M. Kim, Y. Shi, M. Hofmann, D. Nezich, J. F. Rodriguez-Nieva, M. Dresselhaus, T. Palacios, and J. Kong, *ibid.* **12**, 161 (2012).

[22] H. Zeng, C. Zhi, Z. Zhang, X. Wei, X. Wang, W. Guo, Y. Bando, and D. Golberg, Nano Lett. **10**, 5049 (2010).

[23] B. Arnaud, S. Lebegue, P. Rabiller, and M. Alouani, Phys. Rev. Lett. **96**, 026402 (2006); L. Wirtz, A. Marini, M. Gruning, C. Attaccalite, G. Kresse, and A. Rubio, *ibid.* **100**, 189701 (2008); L. Wirtz, A. Marini, and A. Rubio, *ibid.* **96**, 126104 (2006).

[24] S. Ithurria, M. D. Tessier, B. Mahler, R. P. S. M. Lobo, B. Dubertret, and A. L. Efros, Nat. Mater. **10**, 936 (2011).